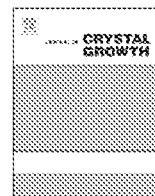


Contents lists available at ScienceDirect

Journal of Crystal Growth

journal homepage: www.elsevier.com/locate/jcrysgr

MBE growth of PbSe thin film with a $9 \times 10^5 \text{ cm}^{-2}$ etch-pits density on patterned (1 1 1)-oriented Si substrate

F. Zhao^a, J. Ma^a, B. Weng^a, D. Li^a, G. Bi^b, A. Chen^c, J. Xu^c, Z. Shi^{a,*}

^a School of Electrical and Computer Engineering, University of Oklahoma, Norman, OK 73019, USA

^b School of Information and Electrical Engineering, Zhejiang University, City College, Hangzhou 310015, China

^c Department of Engineering Science and Mechanics, Pennsylvania State University, University Park, PA 16802, USA

ARTICLE INFO

Article history:

Received 31 December 2009

Received in revised form

25 May 2010

Accepted 27 May 2010

Communicated by E. Calleja

Keywords:

A1. Etch pits

A1. Photoluminescence

A3. Molecules Beam epitaxy

B2. Semiconducting lead compounds

ABSTRACT

PbSe thin film was grown on a patterned Si substrate with (1 1 1)-orientation by molecular-beam epitaxy (MBE). On the mesa, a low dislocation density of $9 \times 10^5 \text{ cm}^{-2}$ was confirmed by the etch-pits density (EPD) wet-etching technique. The photoluminescence (PL) intensity at room temperature from the low dislocation PbSe film was much higher than that from the PbSe film grown on the planar area, which further indicated the high-quality of PbSe thin film grown on patterned Si substrate.

Published by Elsevier B.V.

There is an increasing demand for high quality mid- and long-wave infrared (IR) semiconductor materials grown on Si substrate. One of the applications is for large format long wave infrared imaging system. Existing technologies for mid- and long-wave IR focal plane array (FPA) applications are mainly based on semiconductor photo-detectors. HgCdTe (MCT) is currently the premier material of interest. The best material is produced by molecular beam epitaxy (MBE) on CdZnTe substrates. However, these substrates are costly, brittle and of small size. For applications of large format FPA, many major players are transferring the growth and processes of MCT to alternative substrates, mainly silicon. However, the transfer is complicated by a 19% lattice mismatch and nearly 100% thermal mismatch. The results are a mid- to high- 10^6 cm^{-2} dislocation density, which has deleterious effects on the final FPA. Narrow-band gap lead salt semiconductors have been one of the best candidates for mid-infrared emitters and detectors [1,2]. Recently, lead salt materials such as PbSe and PbSnSe grown on Si substrates have attracted great interest mainly due to their ability to grow on Si substrate for thermal imaging applications in the 3–5 and 8–12 μm atmospheric windows [3–5]. The device-quality PbSe and PbSnSe films have been grown on (1 1 1)-oriented Si substrate with a thin CaF_2 as a buffer layer for compatibility reason between lead salt

materials and Si substrate, which are mainly attributed to the fact that the thermal mismatch strain could relax through dislocation glides along the $\{1 0 0\} \langle 1 1 0 \rangle$ planes [6,7]. Lead salt detector arrays grown on (1 1 1)-oriented Si read-out integrated circuit (ROICs) and two-dimensional (2D) focal-plane array imaging has been successfully demonstrated [4,8]. Because of the large dielectric constant IV–VI Pb-salt materials are much more tolerant to defects in comparison to MCT. Due to this effect Pb-salt materials could have about an order of magnitude higher performance than MCT for the same dislocation density [9]. However, high dislocation densities in the range of low 10^7 to low 10^8 cm^{-2} built up in the epi-layers during growth still limit the device performance. Therefore, reducing the dislocation density of lead salt materials grown on Si substrate is of critical importance for device fabrication.

Thermal annealing from room temperature to high temperatures of about $400 \text{ }^\circ\text{C}$ has been used as an effective method to reduce dislocation density of the epitaxial lead salt films [7,10]. A dislocation density of low 10^6 cm^{-2} on the interior of the rectangular area about $50 \times 70 \mu\text{m}^2$ had been obtained through this thermal annealing technique [7]. Such ex-situ process is, however, trivial and could contaminate the sample. Development of *in-situ* growth method to reduce the dislocation density would be greatly beneficial for devices fabrication.

In this paper, we report a dislocation density of $9 \times 10^5 \text{ cm}^{-2}$ on lead salt thin films grown on patterned (1 1 1)-oriented Si substrate by MBE. To our knowledge, this is the lowest

* Corresponding author.

E-mail address: shi@ou.edu (Z. Shi).

dislocation density of all mid- and long-wave semiconductor materials grown on Si. This result could have significant implications for applications such as large format mid- and long-wave focal plane array, mid-IR lasers on Si and thermal electric devices on Si.

A $1 \times 1 \text{ cm}^2$ single-sided polished (1 1 1)-oriented Si substrate with high resistance ($100 \Omega \text{ cm}$) was patterned and dry-etched by a deep reactive ion etching (RIE) system. Fig. 1 (a) and (b) shows one of such matrices before and after growth with 30° tilted angle, respectively. After dry-etching, the diameter of the holes is $\sim 5 \mu\text{m}$ and spacing from the hole center to center is $\sim 6.5 \mu\text{m}$, the ridge between the patterned holes is about $4.5 \mu\text{m} \times 4.5 \mu\text{m}$, as indicated in Fig. 1 (a). The depth of the hole before growth is $\sim 3 \mu\text{m}$. The patterned Si substrate and another $1 \times 1 \text{ cm}^2$ un-patterned Si substrate were cleaned with a modified Shiraki cleaning method. The un-patterned Si substrate was placed on the center of the substrate holder for *in-situ* reflection high-energy electron diffraction (RHEED) observation and as a reference for

comparison. A custom-designed two-chamber MBE system was used for CaF_2 growth in one chamber and PbSe growth in the other chamber. When the substrate temperature reached 750°C , a clear 7×7 reconstruction RHEED pattern was recorded that indicated the oxidation layer was fully removed. A CaF_2 layer of 2 nm which is within the critical thickness was grown as a buffer layer. PbSe thin films were then grown on the (1 1 1)-oriented CaF_2/Si substrate in another chamber without breaking vacuum using a compound source for PbSe and an elemental source for Se. A 10% Se-to-PbSe flux ratio was used for the growth. The substrate temperature remained at 420°C during the growth. The thickness of the PbSe epitaxial layer was $1.8 \mu\text{m}$ measured on the cross-section of the MBE layer by scanning electron microscopy (SEM). At the bottom and on the side walls of the etched holes, there are polycrystalline-like PbSe deposited. Cross-sectional SEM also shows lateral growth with growth rate of $\sim 10\%$ of the vertical growth along (1 1 1)-orientation. Details of such lateral growth will be discussed elsewhere.

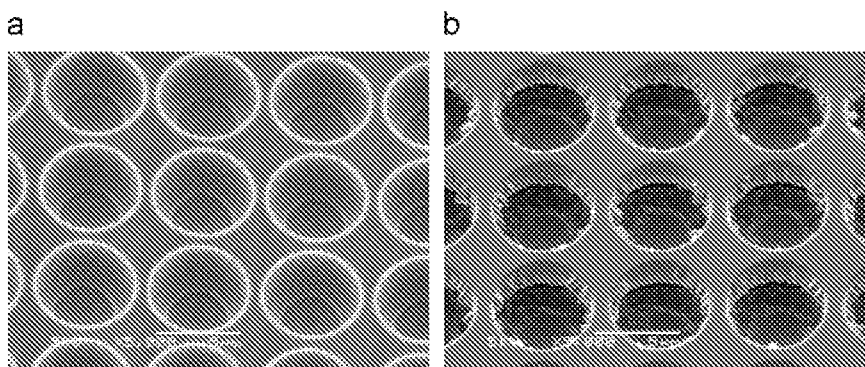


Fig. 1. SEM images (a) before growth and (b) after growth on the patterned (1 1 1)-orientated Si substrate (tilted 30°).

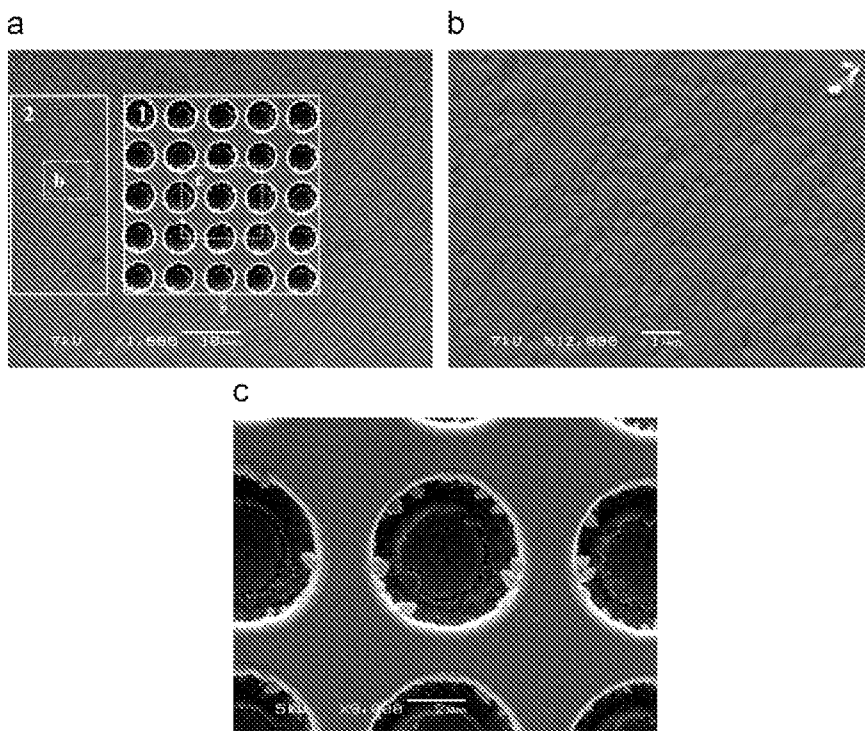


Fig. 2. SEM images from PbSe film on the patterned (1 1 1)-oriented Si substrate after EPD etching: (a) spots for close-up SEM images in area 1 and area 2 as described in the text, (b) close-up SEM in area 2 that shows EPD of about $1 \times 10^8 \text{ cm}^{-2}$ and (c) close-up SEM in area 1 that shows a record low EPD of about $9 \times 10^5 \text{ cm}^{-2}$.

A wet chemical etching process following Ref. [11] was then undertaken to reveal threading dislocations of the PbSe films as etch pits on both patterned and un-patterned substrates. Fig. 2(a) shows SEM images of area 1, where epitaxial layer is on the patterned matrix, and area 2, where epitaxial layer is on the ~ 3 mm un-patterned side of the patterned substrate. Square (b) and square (c) show where close-up SEM images are taken, and are shown in Fig. 2(b) and (c), respectively. In area 2, the revealed threading dislocations are clearly observable in triangle shapes, which is typical for PbSe film grown on (111) substrate due to the three-fold symmetry. The EPD in area 2 is about $1 \times 10^8 \text{ cm}^{-2}$, which is consistent with the result obtained from the PbSe film grown on the un-patterned substrate in the same MBE run. In area 1, however, the EPD is significantly lower. Only one etch pit could be observed in the area shown in Fig. 2(c). Therefore, the EPD in area 1 is calculated to be about $9 \times 10^5 \text{ cm}^{-2}$. To our knowledge, this is the lowest EPD observed for any mid-/long-wave IR materials on Si substrate.

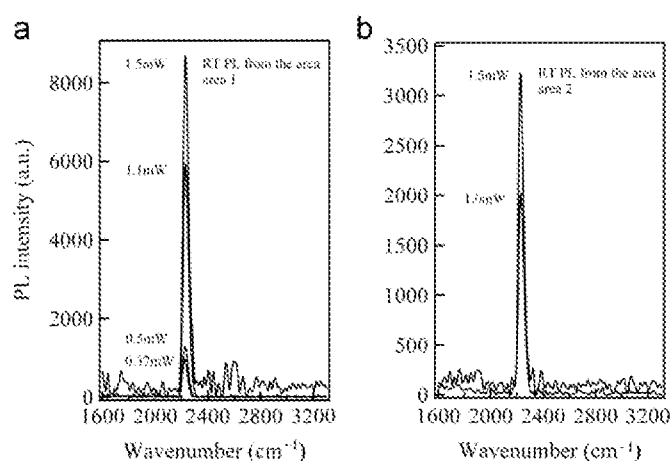


Fig. 3. RT PL spectra from area 1 (a) and area 2 (b) grown on (111)-oriented Si substrate.

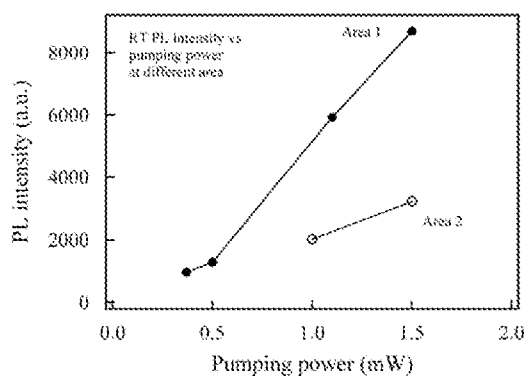


Fig. 4. PL intensity comparison between low EPD area 1 and high EPD area 2.

This result should have significant implications for mid-/long-wave Pb-salt opto-electronic devices on Si substrate.

The samples were also characterized by photoluminescence (PL). The PL was measured with a Bruker IFS 66/S Fourier Transform Infrared (FTIR) spectrometer with step scan function and a PL port. The sample was excited by a $1.064 \mu\text{m}$ pulse Nd:YAG laser. Further details of the setup for optical measurements are given in Ref. [12]. Fig. 3 (a) and (b) shows the room temperature photoluminescence (PL) spectra of area 1 and area 2, respectively. The peak position is 2229 cm^{-1} (276 meV), which showed a typical bulk PbSe behavior. The linewidth is 50 cm^{-1} (6 meV). The pumping power vs PL intensity, shown in Fig. 4, indicates that the PL intensity from low EPD area 1 is about 3 times higher than area 2—another indication of much improved material quality. The focused spot size of the pumping Nd:YAG laser beam on the surface of the sample is about $500 \mu\text{m}$ in diameter. The spacing between two patterned 5×5 matrices is about $55 \mu\text{m}$. Thus, the spot size of the Nd:YAG laser covered six 5×5 patterned matrix. The PL signal from area 1 reflects an average effect of emissions from ridges between the patterned holes and spacing area between the matrices. The effective emission area from area 1 with low EPD is very less than that of the area 2 with high EPD, assuming that emission does not come from the hole area. Based on our experiment, PbSe deposited on the bottom of holes area and on the sidewall are amorphous or polycrystalline. Photoluminescence from such films is typically very weak. Therefore, we believe that the enhanced PL intensity is due to improved material quality on the ridges between the patterned holes.

The lattice mismatch between PbSe and Si substrate is 12.8% at room temperature and the thermal expansion coefficient of PbSe is 7-fold larger than that of Si, as shown in Table 1. Due to such mismatch of lattice constant and thermal expansion coefficients, strains will be introduced during the process of growth and cooling down from growth temperature and room temperature. Since the lateral distance between the patterned holes are small, we tend to believe that for the same strain such reduced lateral distance could help reduce more dislocation by gliding. In addition, the reduced lateral distance could also reduce the dislocation multiplication. These mechanisms for such remarkable dislocation reduction are currently under investigation.

For applications that require full coverage of thin films on the substrate, we propose to grow a thick layer on the patterned Si substrate. The hole area of the patterned substrate is expected to be covered fully by the lateral growth. Such experiment is ongoing and shows some promising results. We will report such lateral growth elsewhere.

In conclusion, PbSe film with a remarkable low dislocation density has been successfully grown on patterned (111)-oriented Si substrate with enhanced PL intensity. This result could lead to significant improvement for IV–VI devices fabricated on Si substrate. It could open doors for many applications on Si substrate such as large format long-wave FPA, mid-IR lasers on Si and thermal electric devices on Si.

Table 1

Lattice constants, thermal expansion coefficient, energy band gap and elastic constants at 300 K.

Material	Lattice constant at RT (Å)	α at 300 K (10^{-6} K^{-1})	Band gap (eV)	Elastic constant (GPa)		
				c_{11}	c_{12}	c_{44}
PbSe	6.126	19.4	0.278	124	19	17
CaF ₂	5.464	19.1	> 5	165	45	34
Si	5.431	2.6	1.17	166	64	79

Acknowledgements

Funding for this work was partially provided by the STTR program of Missile Defense Agency under Contract no. HQ0006-07-C-7657, DoD ARO under Grant W911NF-07-1-0587, NSF DMR-0520550 and by Oklahoma OCAST program under AR082-052.

References

- [1] G. Springholz, Z. Shi, H. Zogg, in: W.K. Liu, M.B. Santos (Eds.), *Thin Films: Heteroepitaxial Systems*, World Scientific, Singapore, 1999.
- [2] D. Khokhlov (Ed.), *Lead Chalcogenides Physics and Applications*, 2002.
- [3] H. Zogg, K. Alchalabi, D. Zimin, K. Kellermann, *Infrared Phys. Technol.* 43 (2002) 251.
- [4] H. Zogg, K. Alchalabi, D. Zimin, K. Kellermann, *IEEE Trans. Electron Devices* 50 (2003) 209.
- [5] G. Vergara, L.J. Gomez, V. Villamayor, M. Alvarez, M.C. Torquemada, M.T. Rodrigo, M. Verdu, F.J. Sanchez, R.M. Almazan, J. Plaza, P. Rodriguez, I. Catalan, R. Gutierrez, M.T. Montojo, *Infrared technology and applications, Proc. SPIE* 6542 (2007) 654220.
- [6] H. Zogg, C. Maissen, S. Blunier, S. Teodoropol, R.M. Overney, T. Richmond, J.W. Tomm, *Semicond. Sci. Technol.* 8 (1993) S337.
- [7] P. Müller, H. Zogg, A. Fach, J. John, C. Paglino, A.N. Tiwari, M. Krejci, G. Kosterz, *Phys. Rev. Lett.* 78 (1997) 3007.
- [8] H. Zogg, A. Fach, J. John, J. Masek, P. Müller, C. Paglino, S. Blunier, *Opt. Eng.* 34 (1995) 1964.
- [9] S. Elizondo, F. Zhao, J. Kar, J. Ma, J. Smart, D. Li, S. Mukherjee, Z. Shi, *J. Electron. Mater.* 37 (2008) 1411.
- [10] H. Zogg, S. Blunier, A. Fach, C. Maissen, P. Muller, S. Teodoropol, V. Meyer, G. Kosterz, A. Dommann, T. Richmond, *Phys. Rev. B* 50 (1994) 10801.
- [11] A. Fach, J. John, P. Muller, C. Paglino, H. Zogg, *J. Electron. Mater.* 26 (1997) 873.
- [12] F. Zhao, H. Wu, L. Jayasinghe, Z. Shi, *Appl. Phys. Lett.* 80 (2002) 1129.